ESTIMATING THE VARIABILITY OF HAMSTRING FUNCTION WITH INCREASING RUNNING SPEED IN OPTIMAL CONTROL SIMULATIONS USING DIRECT COLLOCATION

Carlie J. Ede, Glen M. Blenkinsop and Sam J. Allen

School of Sport, Exercise and Health Sciences, Loughborough University, UK

To investigate the variability in hamstring muscle function, multiple running strides were simulated across a range of running speeds (4 - 9 m/s) using a forward dynamics musculoskeletal model solved using direct collocation (OpenSim Moco). Peak biceps femoris muscle load (force, length, velocity, and power) occurred during the late swing phase, showing variable muscle load across all running speeds. As running speed increased, the time of peak force was consistent at approximately 85% of swing but became less variable in its timing (45 ms [4 m/s] vs 5 ms [9 m/s]). At maximal running speed small changes in variability can result in large changes to muscle function, creating a greater risk of injury and may provide further insight into hamstring strain injuries.

KEYWORDS: musculoskeletal modelling, muscle force, muscle injury, running.

INTRODUCTION: Hamstring strain injury (HSI) is one of the leading causes of injury and time away from many competitive sports (Opar et al., 2012). The majority of HSI's occur at or near maximal running velocity, with the biceps femoris long head (BFlh) the most commonly injured hamstring (HS) muscle, accounting for up to 94% of HSI (Askling et al., 2013). Despite the growing body of research, little change has been observed in the prevalence of HSI, with the mechanisms of injury still not fully understood (Opar et al., 2012). Enhancing the understanding of muscle function during high-speed running is therefore critical in bridging this gap between research and injury prevention. Musculoskeletal (MSK) models offer a valuable tool to non-invasively investigate muscle function. Using these methods, peak hamstring force and strain have been identified during the late swing phase of running (Chumanov et al., 2007; Schache et al., 2012; Thelen et al., 2005) and suggested as risk factors for HSI. While providing important information, these investigations have utilised simplified methods, neglecting activation and tendon dynamics, relying on artificial joint forces, or neglecting the coordination of the entire running stride.

Given the challenging and time-consuming process of simulating high velocity movements, MSK modelling is often applied to a single representative stride, neglecting the possible role of variability on HSI. As an individual approaches maximal speed, small variations in coordination can result in large changes to muscle function, increasing the risk of movements exceeding safe physical limits. Further noted by Chumanov et al. (2007), a 0.1% perturbation to muscle forces resulted in excessive stretch within the BFlh, highlighting the sensitivity to neuromuscular changes and the need to investigate variability, muscle function and HSI.

The emergence and popularity of direct collocation techniques has facilitated the construction of complex and time efficient MSK simulations, with OpenSim Moco providing an accessible and customisable interface to solve a wide range of optimal control problems. Therefore, building on previous work using inverse dynamics (Ede et al., 2020), the aim of this study was to further assess the variability and changes in muscle load across multiple strides and running speeds, using direct collocation through OpenSim Moco. It was hypothesised that muscle load would increase with running speed, and that this would exhibit more stride-to-stride variability.

METHODS: One male participant (age: 28 years, height: 1.83 m, mass: 83.6 kg) completed multiple running trials on an instrumented treadmill (3DI, Treadmetrix, Utah, USA), following informed consent and university ethical approval. Synchronised force (2000 Hz) and 3-D kinematic data (500 Hz, 17 Vantage 5 cameras, Vicon, Oxford Metrics Ltd., Oxford, UK) were recorded. The participant completed three running trials each at 4 m/s, 6 m/s, 8 m/s, and 9 m/s. For each trial, the athlete mounted the treadmill with the belt moving at the desired speed. Once a consistent stride pattern was observed, a minimum of 10 strides were recorded. Sufficient rest was provided between each trial (minimum of 3 mins). To identify when ground

contact occurred, the raw voltage data from the four triaxial force transducers were calibrated and combined to calculate the raw ground reaction force (GRF). The raw voltage data was then filtered during ground contact using a 4th order low pass Butterworth filter (20 Hz), with the flight phase set equal to zero. The GRF, free moment and centre of pressure were then re-calculated from the filtered voltage data.
A generic OpenSim model (Lai et al., 2017), comprising 22 segments, 35 degrees of freedom, 80 muscle-tendon actuators [Hill type muscle (De Groote et al., 2016)] of the lower limbs and 17 ideal torque actuators to control the torso and upper limbs, was scaled to the participant using the OpenSim scale tool. Further adjustments were then made to achieve the desired sprinting task. Specifically, ranges of motion were increased for knee flexion (140° to 150°) and ankle plantarflexion (40° to 75°). Small corrections to the locations of the muscle attachment points (5 ± 3 mm) at the knee were required to produce a suitable moment arm throughout the new range of motion. Subject-specific anthropometric values were used (Yeadon, 1990). The muscle maximum isometric forces were altered based on the muscle volumes from Miller et al. (2021). Optimal fibre lengths (FL) were adjusted so that the torque output matched the angle at maximum isometric force identified by Anderson, Madigan, & Nussbaum (2007), and the maximum contraction velocity was set at 20 fibre lengths per second (FL/s).
Inverse kinematics was performed in OpenSim (v4.3) and the output filtered with the same low-pass filter as the GRF (20 Hz). Each running trial was then divided into 10 individual strides (right leg swing and stance) and the model states and controls solved using direct collocation. OpenSim Moco was used to formulate a tracking problem that minimised the difference between the modelled and experimental joint kinematics, and the muscle effort (sum of the squared excitations). The global foot position was also tracked by minimising the difference between the modelled and measured metatarsophalangeal joint centre. The GRF was included as an external force, applied in the local coordinate system of the toe segments. Each problem consisted of 196 states and 103 controls, first solved on a coarse mesh (2n+1, n = 10), which then served as the initial guess for subsequent mesh refinement, until a mesh interval of ~5 ms (n = 100) was achieved. One trial from each speed was analysed, equating to 10 strides per speed. Each solution was then divided into the stance and swing phases (right leg only) and time normalised (1001 data points to represent 0-100% of each phase) to allow comparison between the various trials. All data was processed using a custom Matlab script (R2018a, MathWorks, MA, USA).

RESULTS: Ten strides for each speed were simulated, though two strides at 4, 6 and 9 m/s failed to converge. Several strides also converged on a local minimum, deemed by kinematic errors that did not reflect a standard running gait, resulting in five solutions for each speed. Each simulation went through four mesh refinements, with an average runtime for the final mesh of 495 mins (± 518 mins) and 207 (± 199) iterations. Kinematic tracking errors displayed an overall RMS of 14.6 ± 4.2 [min: 0.4° (left wrist), max: 5.8° (left ankle)] for all coordinates (1 cm = 1° for the three pelvis translations), averaged across all speeds. As running speed increased, the BFlh generated higher forces, at longer muscle lengths, with greater eccentric loads (Figure 1 and Table 1). During stance, the BFlh acted concentrically, with the peak length, velocity, force, and power occurring close to initial ground contact (Figure 1). During swing, the BFlh first shortened, before reaching peak length in the last quarter (81% ± 3%) of the swing phase. Peak eccentric fibre velocity increased from 4.4 FL/s (4 m/s) to 10.6 FL/s (8 m/s). BFlh peak force remained similar between 4 m/s and 6 m/s but increased markedly at 8 m/s and further still at 9 m/s (Table 1). Muscle power and negative work also showed large increases with running speed, resulting in a high eccentric demand during terminal swing. Across speeds, stride-to-stride variability displayed no distinct pattern, with peak muscle force showing the lowest, but velocity the highest variability at 8 m/s. (Table 1). Alternatively, peak muscle force occurred at 85% (± 1.2%) of swing but became less variable in its timing [4 m/s: 84.2% ± 9.6% (± 45 ms), 9 m/s: 84.3% ± 1.7 % (± 5 ms)].

Table 1: Mean ± std muscle variables of the biceps femoris long head during swing at different running speeds. Positive velocity (lengthening), Negative power (eccentric).

	Length at peak force (FL)*	Force (N)	Velocity (FL/s)*	Power (W)	Work (J)
4 m/s	0.80 ± 0.03	904 ± 230	4.40 ± 0.24	-161 ± 101	-17 ± 9
6 m/s	0.96 ± 0.03	933 ± 315	7.36 ± 0.68	-210 ± 99	-20 ± 9
8 m/s	1.04 ± 0.03	1130 ± 147	10.57 ± 1.63	-281 ± 41	-23 ± 6
9 m/s	1.06 ± 0.03	1515 ± 206	10.01 ± 1.10	-427 ± 81	-36 ± 10

* FL = normalised to optimal fibre length

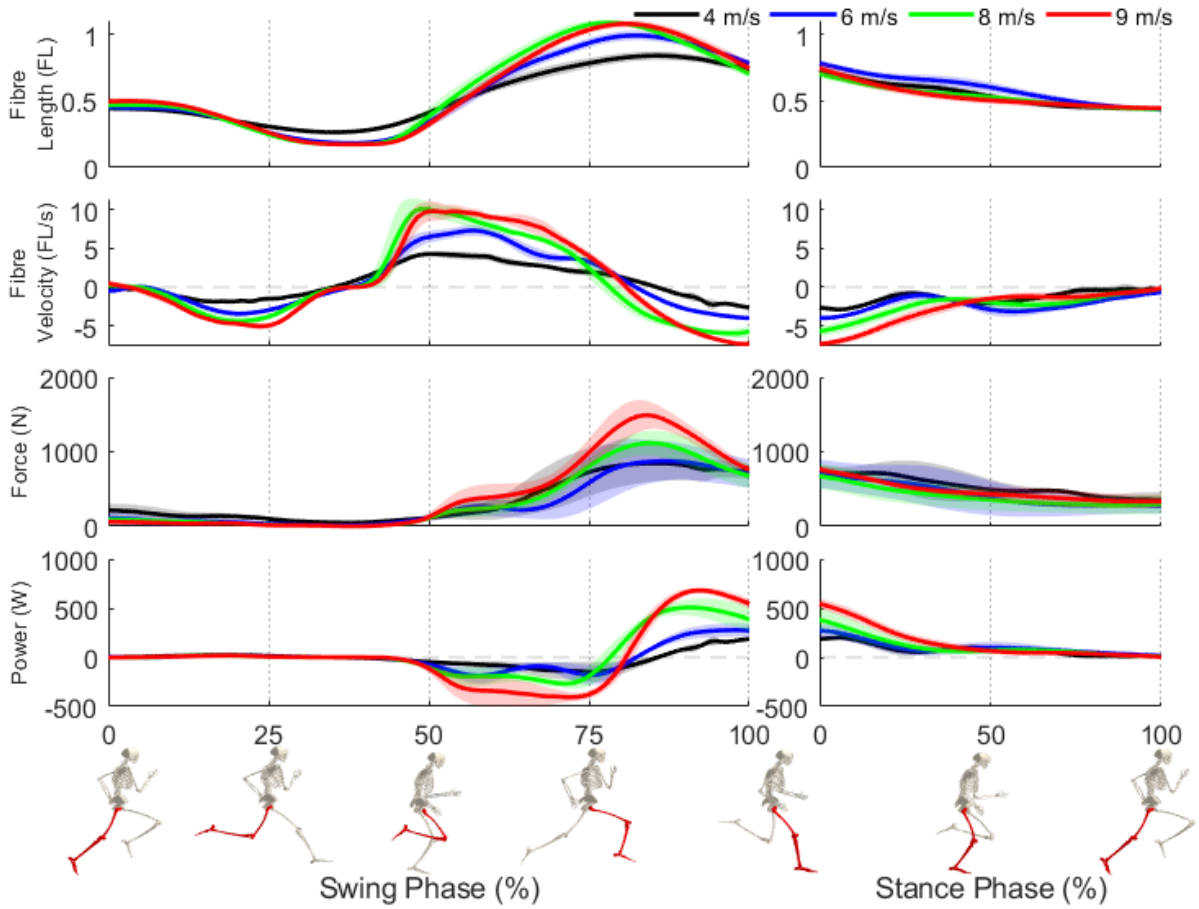

Figure 1: Biceps femoris long head normalised muscle fibre length and velocity, muscle force and power (from top to bottom) for different running speeds. Solid lines show the average of all strides with the standard deviation (shaded area). Positive velocity (lengthening), Negative power (eccentric).

DISCUSSION: The aim of this study was to assess the function and variability of the BFlh during running across multiple strides and speeds using a forward dynamic MSK model solved using direct collocation, incorporating activation and muscle dynamics to overcome limitations of past work (Ede et al., 2020). In agreement with previous studies (Chumanov et al., 2007; Schache et al., 2012), the peak BFlh load (length, velocity, force, and power) increased with running speed, working concentrically during stance, and displaying a high eccentric demand during terminal swing (Figure 1 and Table 1). In contrast to the hypothesis, variability in muscle loads displayed no consistent pattern (Table 1). Though, in line with previous work, the timing of the peak force became less variable as running speed increased, reducing the time window at which peak force occurred.

The peak muscle force (18.13 N/kg, 9 m/s) showed good agreement to that reported by Thelen et al. (2005) (17.6, N/kg, 9.3 m/s), though it is lower than those reported by Schache et al. (2012) where static optimisation was used (26.35 N/kg, 8.95 m/s). Peak force was also shown to occur later in the swing [85 % vs 57% (Schache et al., 2012)], likely due to the inclusion of activation and tendon dynamics in the present study. The timing of peak force appeared independent of running speed, but occurred at longer muscle lengths, and became less variable in its timing (Figure 1 and Table 1). Increased variability, as a result of coordination errors or external factors could result in the muscle exceeding this range, leading to injurious situations and warranting further investigation. In the future, exploring these situations through the use of predictive simulations may provide further insight into HS function and risk of HSI.
MSK modelling is a powerful tool that can provide insight into muscle function, but limitations of the study must be considered when evaluating the results. Specifically, a measured GRF was applied to the model, rather than calculated using a foot-ground contact model. The measured force may have included artifacts from the vibrations of the instrumented treadmill and subsequent processing. Despite this, the estimated muscle function is consistent with previous work, giving confidence in the current results.

CONCLUSION: The results of this study showed peak muscle length, velocity, force, power, and negative work increased with running speed, placing significant stress on the BFlh during the late swing. As running speed increased, the timing of peak muscle force became more consistent, but occurred at longer muscle lengths. Such that, small changes in coordination may expose the HS to suboptimal or injurious situations. The estimation of muscle function during cyclical high-speed movements via MSK simulations can help to understand and possibly avoid muscular injuries, with the application of direct collocation using OpenSim Moco facilitating the investigation of more complex and dynamic tasks in future.

REFERENCES:

Anderson, D. E., Madigan, M. L., & Nussbaum, M. A. (2007). Maximum voluntary joint torque as a function of joint angle and angular velocity: model development and application to the lower limb. *Journal of Biomechanics*, *40*(14), 3105–3113.

Askling, C. M., Tengvar, M., & Thorstensson, A. (2013). Acute hamstring injuries in Swedish elite football: a prospective randomised controlled clinical trial comparing two rehabilitation protocols. *British Journal of Sports Medicine*, *47*(15), 953–959.

Chumanov, E. S., Heiderscheit, B. C., & Thelen, D. G. (2007). The effect of speed and influence of individual muscles on hamstring mechanics during the swing phase of sprinting. *Journal of Biomechanics*, *40*(16), 3555–3562.

De Groote, F., Kinney, A. L., Rao, A. V., & Fregly, B. J. (2016). Evaluation of Direct Collocation Optimal Control Problem Formulations for Solving the Muscle Redundancy Problem. *Annals of Biomedical Engineering*, *44*(10), 2922–2936.

Ede, C., Blenkinsop, G., & Allen, S. J. (2020). Does Variability Play a Role in Hamstring Strain Injuries? A Pilot Study in Sprinting. *ISBS-Conference Proceedings Archive*, 416.

Lai, A. K. M., Arnold, A. S., & Wakeling, J. M. (2017). Why are Antagonist Muscles Co-activated in My Simulation? A Musculoskeletal Model for Analysing Human Locomotor Tasks. *Annals of Biomedical Engineering*, *45*(12), 2762–2774.

Miller, R., Balshaw, T. G., Massey, G. J., Maeo, S., Lanza, M. B., Johnston, M., Allen, S. J., & Folland, J. P. (2021). The Muscle Morphology of Elite Sprint Running. *Medicine and Science in Sports and Exercise*, *53*(4), 804–815.

Opar, D. A., Williams, M. D., & Shield, A. J. (2012). Hamstring strain injuries: Factors that Lead to injury and re-Injury. *Sports Medicine*, *42*(3), 209–226.

Schache, A. G., Dorn, T. W., Blanch, P. D., Brown, N. A. T., & Pandy, M. G. (2012). Mechanics of the human hamstring muscles during sprinting. *Medicine and Science in Sports and Exercise*, *44*(4), 647–658.

Thelen, D. G., Chumanov, E. S., Best, T. M., Swanson, S. C., & Heiderscheit, B. C. (2005). Simulation of biceps femoris musculotendon mechanics during the swing phase of sprinting. *Medicine and Science in Sports and Exercise*, *37*(11), 1931–1938.

Yeadon, M. R. (1990). The simulation of aerial movement-II. A mathematical inertia model of the human body. *Journal of Biomechanics*, *23*(1), 67–74.